

DAVIS-Ag: A Synthetic Plant Dataset for Developing Domain-Inspired Active Vision in Agricultural Robots

Taeyeong Choi^{1,4}, Dario Guevara^{2,4}, Grisha Bandodkar¹, Zifei Cheng¹,
Chonghan Wang¹, Brian N. Bailey³, Mason Earles^{2,4}, and Xin Liu^{1,4}

Abstract—In agricultural environments, viewpoint planning can be a critical functionality for a robot with visual sensors to obtain informative observations of objects of interest (e.g., fruits) from complex structures of plant with random occlusions. Although recent studies on active vision have shown some potential for agricultural tasks, each model has been designed and validated on a unique environment that would not easily be replicated for benchmarking novel methods being developed later. In this paper, hence, we introduce a dataset for more extensive research on *Domain-inspired Active VISION in Agriculture (DAVIS-Ag)*. To be specific, we utilized our open-source “AgML” framework and the 3D plant simulator of “Helios” to produce 502K RGB images from 30K dense spatial locations in 632 realistically synthesized orchards of strawberries, tomatoes, and grapes. In addition, useful labels are provided for each image, including (1) bounding boxes and (2) pixel-wise instance segmentations for all identifiable fruits, and also (3) pointers to other images that are *reachable* by an execution of action so as to simulate the active selection of viewpoint at each time step. Using DAVIS-Ag, we show the motivating examples in which performance of fruit detection for the same plant can significantly vary depending on the position and orientation of camera view primarily due to occlusions by other components such as leaves. Furthermore, we develop several baseline models to showcase the “usage” of data with one of agricultural active vision tasks—fruit search optimization—providing evaluation results against which future studies could benchmark their methodologies. For encouraging relevant research, our dataset is released online to be freely available at: <https://github.com/ctyeong/DAVIS-Ag>

I. INTRODUCTION

For precision agriculture, accurate perception is an essential functionality for robots to identify the maturity or health statuses of plants. One of the challenges is, however, caused by the wild environments, in which various objects such as fruits, stems, and leaves can be only partially visible due to occlusions by one another [1]. Consequently, a diseased fruit could be misclassified as a normal instance more easily when anomalous parts are not fully visible [2]. Also, yield estimation can be inaccurate, if a crop detector cannot access the views to some of occluded individuals [3].

As a potential solution, “active vision” approaches [4] have recently been developed, in which an embodied agent plans its motion sequence to gain more informative viewpoints around plants. More specifically, a robotic arm with some

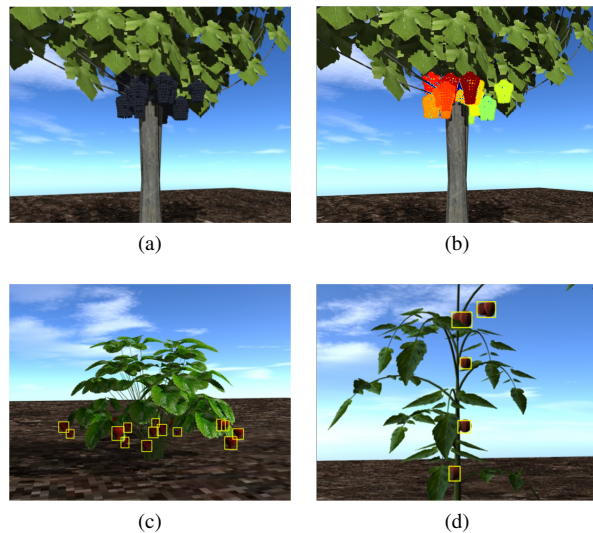


Fig. 1: Example images from single-plant scenarios of DAVIS-Ag: (a)–(b) goblet vine, (c) strawberry, and (d) tomato. Labels for fruits are also visualized with bounding boxes in (c)–(d), and instance segmentation of (a) in (b).

camera sensor on it is often deployed to move effectively while maximizing the area coverage of fruit to potentially classify its maturity [5], [6], predict the size and pose information [7], or reconstruct the 3D structures of parts of focal plant [8], [9], [10]. However, every model has been built up on a uniquely customized environment with either simulation or physical setups that could not be easily replicated without technical familiarity when new studies try to benchmark their novel approaches.

To bridge the gap, in this paper, we introduce an easy-to-access dataset, so-called *Domain-inspired Active VISION in Agriculture (DAVIS-Ag)*, which contains over 502K HD-quality RGB images gathered from 30K sampling locations with various camera angles to obtain diverse viewpoints around realistically simulated plants (cf. Fig. 1). Inspired by some of existing datasets for non-agricultural applications [11], [12], DAVIS-Ag also provides the pointers between reachable viewpoints by possible actions (i.e., *forward*, *backward*, *left*, *right*, *rotate*, *up*, *down*, etc.) to enable it to simulate sequences of motions of embodied agent with a RGB camera. Moreover, useful visual labels—i.e., bounding box and instance segmentation—of every observable fruit (Fig. 1) are included so the future research in agricultural

¹Department of Computer Science, ²Department of Biological and Agricultural Engineering, ³Department of Plant Sciences, and ⁴AI Institute for Next-Generation Food Systems (AIFS) at the University of California, Davis, USA. {tae Choi, dguevara, gbandodkar, zfcheng, wchwang, bnbailey, jmearles, xinliu}@udcavis.edu

active vision could immediately utilize the dataset without additional efforts for annotating it.

To be specific, we fully utilized our “AgML”¹ framework—a comprehensive open-source Python library for agricultural AI research—to interface with Helios [13], which can create visually realistic plants in 3D based on mathematically modeled environmental factors such as radiation transfer, surface energy balance, and photo synthesis among others. Consequently, we could generate a novel dataset that includes images of plants with a high degree of realistic variations, whereas existing datasets for active vision research have focused largely on typical everyday items in indoor scenes (e.g., living room). To the best of our knowledge, DAVIS-Ag is the first public dataset purposed to assist in active vision research particularly in agricultural domains. Also, we show some experimental results with the data to present baseline performances on one of the agricultural active vision tasks (i.e., fruit search) to promote more future studies in the field.

II. RELATED WORK

In this section, we discuss relevant studies on robotic active motion for perception first in more general, non-agricultural scenarios and then in agricultural applications.

A. Active Vision for Non-Agricultural Applications

Active vision has been broadly studied for decades in robotics [4], and it includes subfields of various tasks, such as classification [14], [15], detection [16], and manipulation [17] of objects, segmentation [18] and reconstruction [19] of scenes, and also searching for certain items in environments [20], [21]. Though objective functions can differ depending on the scenario, the same goal is essentially pursued to optimize the next poses of agent with visual sensors to gain the most useful information.

In particular, our suggested tasks with DAVIS-Ag are most relevant to “active object detection” [16], [22] for precise prediction of yield or robotic picking of fruits detected. In contrast to the existing setups namely with indoor environments (e.g., home service robot [23]), ours is, however, designed for exploration in agricultural *outdoor* fields. Also, objects under consideration in agricultural contexts, such as fruits, leaves, and stems, are significantly different from those in other domains in visual elements, such as shape, color, etc.

1) *Table-top Datasets*: Datasets with various settings have been released to keep promoting related research in practical scenarios by curating images captured from different viewpoints. For instance, T-LESS [24], BigBIRD [25], and ROBI [26] each provide RGB images along with depth data of a single or multiple objects arbitrarily posed on a *turnable* over which cameras were systematically moved to obtain the view at each point of a spherical grid while imitating possible motions of an robotic arm. Our single-plant scenarios in DAVIS-Ag are also designed to simulate a mobile robot around a target plant at the center of field. Still, our dataset

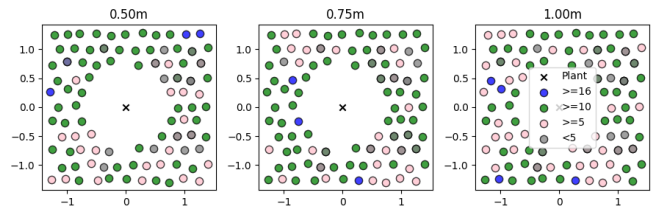


Fig. 2: Numbers of visible strawberries at different positions in a 3D example environment with the single plant at the center in which 24 fruits existed in total. In particular, three levels of height were considered: 0.50m, 0.75m, and 1.00m.

is distinct in that even same species of fruits or plant may appear *differently* in size or shape in a probabilistic manner at each time of realistic synthesis, while the existing non-agricultural data sets were mostly acquired from the rigid, commercialized items of prefixed sizes or designs depending on the category (e.g., eye bolt, bottle, etc.).

2) Datasets & Simulators for Scene Understanding:

Similar to DAVIS-Ag, Active Vision Dataset (AVD) [11] and Real 3D Embodied Dataset (R3ED) [12] both also offer not only bounding boxes of objects in each image but the links between densely sampled viewpoints if they are reachable by an application of one of six actions—i.e., forward, backward, left, right, rotate clockwise, and rotate counterclockwise—to simulate an exploratory robot in a scene.

Yet, ours includes “vertical” translations such as up and down as well to emulate freer motions in agricultural open fields, which might be particularly useful to avoid occluders through highly complex structures of plant. Also, we add some level of additive white noise to the positions of camera to consider possibility of “slips” of robot in an unfavorable condition of terrain, while AVD [11] and R3ED [12] do not intentionally take this into account in their indoor navigation.

More recently, photorealistic 3D simulators (e.g., Habitat 2.0 [27]) have been introduced to enable virtual embodied agents to interact with physics-engine-based environments which also offer realistic visualizations. However, DAVIS-Ag is a pre-computed dataset that presents all possible visual inputs from spatial exploration so researchers can skip computationally expensive processes for 3D rendering and annotation but instead focus only on developing novel methods.

B. Active Vision in Agriculture

In agriculture, active vision has been investigated to better monitor statuses of plants, localize fruits for robotic picking, or predict potential yields under significantly cluttered environments. For example, dynamic viewpoint-decision systems were developed to strategically move a robotic arm to accurately estimate the maturity [6] or the size [9] of partially visible fruit. Also, maximizing the viewed area of target fruit has been studied to closely examine the instance as well as provide a manipulator with useful information for picking [5], [9]. For similar motivation, Menon et al. [10] used active motions of a robotic arm with a sensor to

¹<https://github.com/Project-AgML/AgML>

	Strawberry	Tomato	Goblet Vine
Plant/Trunk Height	40	100	70
Fruit Radius	2.5	3	0.75
Leaf Length/Width	10	20	18
Camera Altitudes	25, 40, 55	70, 110, 150	50, 75, 100

TABLE I: Top three rows show the default values of parameters for plant generation in Helios, in which the fruit radius of vine refers to that of individual berries. The last row reveals the three camera heights considered for each orchard type. Every value is in units of centimeters.

reconstruct the hidden structure of fruit under another object. In addition, full 3D reconstruction of entire plant also has been performed in the context of active vision [8], [28].

Nonetheless, absence of a common testbed—such as ones described in Section II-A.1 and Section II-A.2—has been a challenge to evaluate a method against another in agricultural applications. For instance, for simulation, most of used platforms have been implemented based upon V-REP [29], Panda3D [30], or Robot Operating System (ROS) [31] with Gazebo [32] which are specially customized for each research problem. In this paper, on the other hand, we propose DAVIS-Ag, which does not require technical familiarity with any of those for using it, while it features $> 502K$ RGB images sampled from 632 simulated plant environments along with the labels such as bounding boxes and fruit-instance segmentation, which could be useful for various agricultural tasks.

III. DATA SYNTHESIS & COLLECTION

This section describes more technical details on our pipeline of simulation and the procedure of data collection.

A. 3D Plant Simulation

Our data synthesis framework is based upon our open-source project, so-called AgML, which is a comprehensive Python library to support machine learning research for agricultural applications. In particular, the generation of the synthetic data was conducted with the *synthetic* module, which allows to communicate with the C++ API’s of Helios [13]—a 3D plant and environment modeling framework, which can create semi-random tree geometries [33] to provide a more realistic variability of crops.

More specifically, we configured AgML to utilize several useful plugins of Helios as below:

- *Canopy Generator*: Synthesized three kinds of crops, including goblet vines, strawberries, and tomatoes (cf. Fig. 1), varying their sizes of fruit, leaf, and trunk within the ranges of $\pm 20\%$, $\pm 20\%$, and $\pm 15\%$ from the default settings in Table I.
- *Visualizer*: Generated high-quality RGB images of 1280×720 in resolution from simulated camera positions densely distributed across the field, discussed with more details in Section III-B.
- *Synthetic Annotation*: Produced fruit-focused labels in each image such as (1) 2D coordinates of bounding

	Step Size	# of Alt.	# of Ang.	# of Act.	# of Img.
Single-plant	25cm	3	1	6	285 ~ 348
Multi-plant	50cm	2	12	8	1, 128 ~ 1, 800

TABLE II: Left four columns show the settings for SP and MP scenarios, including the numbers of camera altitudes and angles. Also, the right-most column indicates the number of images per virtual farm in each scenario.

boxes (Fig. 1d) and (2) pixel-wise instance segmentation for fruits (Fig. 1b).

In the following sections, we explain more specific settings employed for those modules to construct useful data composition in DAVIS-Ag.

B. Two Scenarios & Camera Poses

For each kind of plant, we particularly consider two types of scenarios—i.e., “single-plant” (SP) and “multi-plant” (MP)—with the camera settings in Table II. To be specific, in SP, each camera view is set up to always aim at the plant at the origin regardless of its spatial position, with a reasonable assumption that tracking a single plant target to maintain it within the view can be easily implemented. Thus, the possible actions include *forward*, *backward*, *left*, and *right* along with *up* and *down*, which control the altitude of viewpoint among three plant-specific options in Table I.

On the other hand, MP uses three plants in a single row for both tomato and goblet vine cases while strawberry examples each involve five plants in a row. Also, the RGB images are sampled every 30 degrees at each position as in [11], and consequently, *rotate_clockwise* and *rotate_counterclockwise* are added to the action set. To compensate for this increased computational load in data collection, we set the sampling resolution to be slightly coarser by doubling the step size from 25cm [12] to 50cm and considering only two levels of camera altitudes—i.e., the highest and the lowest.

As in Fig. 2, contrary to existing datasets [11], [12], we also use an additive white Gaussian noise with a standard deviation of 2.5cm to each x, y -coordinate of camera position to simulate a robot that might “slip” to some degree potentially due to a harsh terrain condition in outdoor environments. Also, the spatial sizes of grid in the two scenarios are set up differently—i.e., $3m \times 3m$ for SP and $7m \times 3m$ for MP—to keep the space to be sufficiently large for exploration while considering computational costs for simulation.

C. Labels & Potential Applications

DAVIS-Ag offers the labels below for each RGB image:

- 2D bounding boxes with unique ID’s of associated fruits (Fig. 1d).
- Pixel-wise instance segmentation for every fruit (Fig. 1b).
- Pointers to other images of viewpoints reachable by an action.
- Pose of the camera denoted as (x, y, z, ψ, θ) based on the global coordinate system, where (x, y, z) represents

Scenarios	Strawberry		Tomato		Goblet Vine	
	SP	MP	SP	MP	SP	MP
# of Scenes	86	77	130	113	182	44
# of Images	24, 510	86, 856	45, 240	203, 400	63, 336	79, 200

TABLE III: Detailed specifications of DAVIS-Ag for each type of plant.

the position in three-dimensional space while ψ and θ are the yaw and the pitch of camera, respectively.

Bounding boxes around observed fruits are generally useful for building fruit detectors for yield estimation [3], robotic picking, or health monitoring. In particular, identifying individual crops [34] could also be developed from the labels of instance ID. Similarly, instance segmentation could also be useful to find the specific examples of occluded fruit so that a robot could learn an active maneuver to lead better views for “fruit coverage” [5], [35], which infers poses or sizes of individual fruits. In addition, each RGB image in our dataset is associated with a tuple of (x, y, z, ψ, θ) based on the global coordinate system, which may also be used to validate a framework for “visual localization” [36] in agricultural environments. “Vision-based navigation” may also be investigated with the dataset to build a robot to arrive in a particular view by only relying on a RGB camera. Though DAVIS-Ag is a set of still images, all these applications on *motional* capabilities of robot can be explored because it presents the “view-to-view” pointers with associated actions.

In particular, we discarded unreasonably small bounding boxes or ones that cover mostly occluded instances by using manually determined threshold on the minimum number of pixels belonging to a fruit—i.e., 210, 240, and 700 for a strawberry, a tomato, and a grape, respectively. Furthermore, if a particular action leads to a location either outside the grid or overly close to a plant (e.g., $< 75\text{cm}$ for strawberry and $< 100\text{cm}$ for others), it is regarded as an invalid action to connect to no image.

D. Data Specification

With all aforementioned considerations, we produced DAVIS-Ag, which contains $> 502\text{K}$ images from over 632 virtual farms. In other words, our dataset provides magnitudes more RGB images than some state-of-the-art benchmark datasets such as AVD [11]. More details of specification are presented in Table III.

IV. MOTIVATING EXAMPLE

Here, we use a representative instance of simulated plant environment to show that active viewpoint planning can considerably impact performances in agricultural tasks that would particularly require clear visibility to a certain type of object (e.g., fruit). Specifically, as in Fig. 2, we examined the numbers of visible strawberries from different viewpoints in a field where a single plant with 24 fruits are located at the center of a grid. All configurations for the poses of deployed camera and the environmental settings in this *single-plant* scenario followed the details in Section III-B.

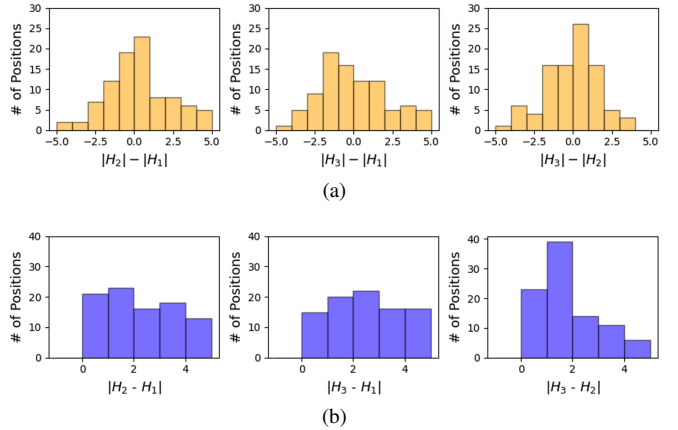


Fig. 3: (a) Histograms of different numbers of observed strawberries from various altitudes $z_1 < z_2 < z_3$ at the same x, y positions. (b) Histograms of numbers of newly found instances at higher altitudes. All were obtained from the example used in Fig. 2. H_k denotes a set of observable fruits at height z_k .

Figure 2 visualizes dramatic difference in visibility of fruits depending on the camera location; for example, the number of seeable fruits can significantly vary from < 5 to ≥ 16 simply by repositioning the camera only several steps away. Similarly, even at the same location, using a higher or lower view can also bring about the change to the visibility (cf. Fig. 3a), and also, none of the spots provided the viewpoint that can cover all of 24 strawberries at once.

These observations imply that (1) plant environments are basically highly unstructured even with this simplified scenario, and thus, (2) application of *active vision* can greatly benefit autonomous systems for monitoring the whole plants or fruits. The latter is also advocated by Fig. 3, which shows that though lower views tend to show more strawberries (Fig. 3a), higher ones can still lead to the encounters with novel instances (Fig. 3b). Hence, strategically choosing viewpoints needs to be considered to precisely understand an agricultural environment from perceived information. Our proposed dataset is designed to further encourage relevant research by providing a large amount of realistic plant images with visual and spatial annotations.

V. EXPERIMENTS

In this section, we show a use case of DAVIS-Ag dataset to build a solution to a particular agricultural problem. To be specific, fruit search optimization is first introduced as a main task for the following experiments, and then, the quantitative and qualitative results from several tested methods are discussed.

A. Fruit Search Optimization

DAVIS-Ag can be utilized for exploring various active vision tasks. In this experiment, we particularly investigate fruit search optimization (FSO), which is for a robot to optimize its sequential motion of a certain length ℓ to observe

or scan as many individual fruits in the field as possible. FSO could be regarded as a sub-task of yield prediction and fruit monitoring, which generally require a robot to encounter every individual instance.

To focus on the performance solely from motion planning, we here design our experiments with an assumption that a near-perfect vision system is available. That is, a robotic agent can be fed with true bounding boxes of visible fruits. Still, strategic motions must be generated to clear non-fruit objects and already counted instances from the view to discover more unseen ones.

For evaluation, “search score” after ℓ steps is calculated:

$$s_\ell \triangleq \frac{n_\ell^{\text{seen}}}{n^{\text{total}}}, \quad (1)$$

which is the ratio of seen fruits against all instances present in the explored farm, so the range is between 0 (worst) and 1 (best) to evaluate the result. In particular, we set ℓ to be 5 and 10 for SP and MP scenarios in our experiments, respectively.

B. Employed Algorithms

For solving FSO, we test three heuristic approaches and a reinforcement learning (RL) [37] method which are all designed to select actions $a_t \in A$ to find more individual fruits. More details of each algorithm are described below:

- Random (Rand): Choose a random action a_t by a uniform distribution over possible actions
- To-More (TM): Inspired by [6], partition the RGB image into three regions—i.e., left, center, and right. Then, pursue the region that displays more fruit bounding boxes. Take *left* (*right*) for the left (right) region, and *forward* for the central.
- To-Less (TL): Behave in the opposite way to TM by moving to the region with less fruits.
- DQN [38]: Deep Q-Network, a RL method using a deep convolutional neural network which only relies on RGB images as input.

TM is adopted with the intuition that fruits may form as a cluster within a distance, whereas TL is to expect discovering novel instances from the unexplored region. Also, TM and TL both use a random action at times when their choice of action would lead out of the grid.

Similarly, after training, the DQN applies a greedy policy that chooses the action with the highest Q-value estimation, but if it does not connect to a valid viewpoint in the grid, an alternative with the next highest Q-value is used. Also, for RL, reward r_t is set to 1 if at least one new fruit instance has been sensed by taking an action a_t , and $r_t = 0$ otherwise.

Moreover, the network is composed of four convolutional layers with 32, 64, 64, and 128 (3×3) kernels followed by two fully-connected layers with 64 and $|A|$ nodes, respectively, where A is the set of possible actions. In particular, twice more convolutional kernels are adopted for MP tasks to effectively handle the more complex settings. Also, each input $\mathcal{I} \in \mathbb{R}^{w \times h \times 3\ell}$ is obtained by concatenating the RGB images from the latest ℓ steps along the last dimension to consider historical information, where w and

Scenarios Time Step	Strawberry (SP)			Goblet Vine (MP)			
	1	3	5	1	4	7	10
Rand	.257	.307	.313	.066	.084	.105	.114
To-More	.294	.400	.434	.074	.094	.105	.108
To-Less	.310	.409	.457	.078	.097	.100	.106
DQN	.239	.363	.479	.061	.098	.126	.155

TABLE IV: Average search scores of tested methods for two different scenarios with strawberries and goblet vines. Highest scores at each time step are in bold.

h are the shortened width and height set to 64, respectively. Our Python codes for all applied methods are also accessible online along with the dataset.

C. Results

Here, we showcase DAVIS-Ag as a useful platform of agricultural active vision research by presenting our experimental results in two representative scenes—single-plant strawberries and multi-plant goblet vines. We choose these since they are particularly challenging due to severe occlusions by (1) leaves and stems over relatively small strawberries or (2) a densely layered cluster of neighboring grapes.

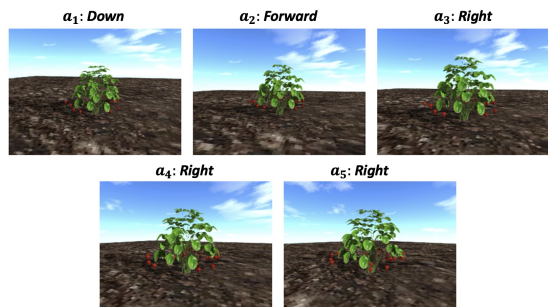
In every experiment, a split is applied to gain 70% and 30% data for training and test particularly for DQN. For fair comparison, all other methods are also performed only on the same test data. In addition, for each scene from the test set, the agent is evaluated five times in total while it is spawned at a random initial pose for each run.

1) *Single Strawberry Plant*: We first explore the SP case with strawberries to maximize the search score in Eq. (1) for SFO. As shown in Table IV, any method could not gain over .500 by any chance, and it suggests that the task is not trivial. Nevertheless, every method generally benefits from taking more steps to increase the likelihood of observing novel fruits. The random policy, however, achieves the worst performance among others at last steps implying that more carefully selected actions from other models demonstrate their better *qualities* leading to informative observations.

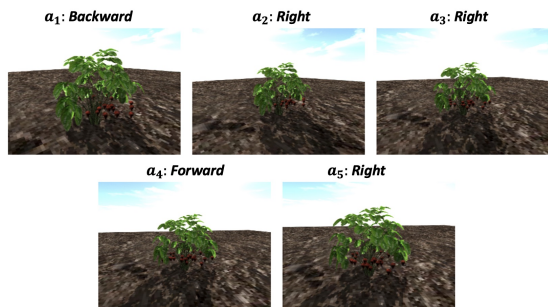
Also, the results from the To-More and To-Less heuristics support our hypothesis that the spatial distribution of currently visible fruits could be a useful cue for decision making, since it outperforms the random selection by a large margin. In particular, the To-Less approach showed the best performance compared to others until the exploration process has ended at the third time step.

The naïve DQN algorithm eventually obtained the highest score after all five steps. Interestingly, it did not show any significant result at initial steps even showing the worst performance after the first action. However, its highest score at the last time step implies that the first seemingly unwise actions were learned for the purpose of exploration to finally optimize the whole sequence of viewpoints.

Figure 4 visualize two observation-action trajectories that the DQN agent presented in one of the test environments after training. As can be seen in those examples, the trained agent appears to frequently take the “right” action in many cases to naturally revolve around the plant in that particular



(a)



(b)

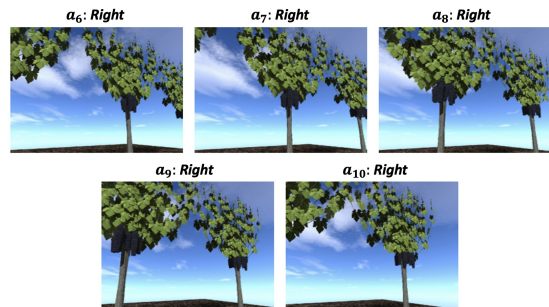
Fig. 4: Five-step action sequences of the trained DQN in two different environments with single strawberry plants. Brightness has been adjusted for clarity.

direction. Another discovered pattern is that if the initial viewpoint is at a high position, it would be preferred to *decrease* the altitude as shown in Fig. 4a. The benefit of such a behavior could be advocated by our findings with Fig. 3a, which shows that more strawberries may be seen at a lower height in general. Also, the robot learned to maintain a particular degree of *distance* to the plant by using the forward or backward action. In particular, the agent tries to move toward the focal plant, if fruits could become too small to recognize by taking any other action.

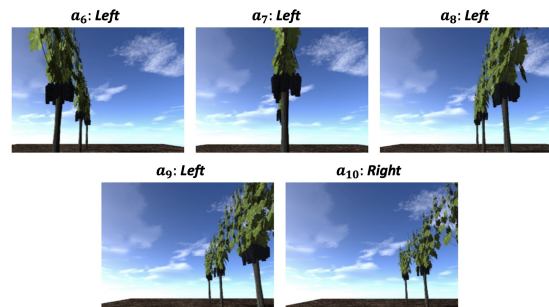
We claim that more advanced AI algorithms could be adopted to achieve better results with discoveries of more effective and adaptive motions. For example, combinations with the “up” action could also be useful in some situations to view novel fruits, while it often leads to less observations.

2) *Multi-Goblet Vine Scenario*: We evaluate the four methods also on goblet vine data under MP setting. Poor performances ($< 16\%$) in Table IV indicates higher difficulty than the SP task because a more complex plan needs to be devised considering (1) more trees in a larger area, (2) a twice longer mission time, and (3) two more available actions (“rotate clockwise” and “rotate counter clockwise”).

Nonetheless, DQN still shows its superiority to others. In particular, as in the previous experiment, the performance at initial steps is not significantly different from other methods. However, at later steps, the learned policy presents more useful actions to lead to the highest coverage of existing fruits. More powerful networks such as LSTM could improve the performance by better incorporating historical observations.



(a)



(b)

Fig. 5: Last five action selections of DQN in two separate environments with multiple goblet vines.

Surprisingly, the behaviors of our bounding-box-based heuristics—To-More and To-Less—worsened significantly. Their final scores are even lower than the random selection approach, and one of the main reasons could be the ignorance of rotation actions by design. With those included possibly using more partitions for action selection, a better performance could be obtained.

Figure 5 shows the action sequences of DQN in two tested vineyards after training. We observed that the trained agent initially uses arbitrary motions especially if trees are not in its view, but it later tries to move along (Fig. 5a) or cross (Fig. 5b) the row, once some trees have been seen. This is a reasonable approach since the trees are positioned linearly in those environments. If more time steps are allotted, more creative motion plans could be learned to see hidden individual fruits under clusters of others as in Fig. 1b.

VI. CONCLUSION & FUTURE WORK

We have proposed DAVIS-Ag, a novel dataset for developing effective active vision methodologies in agricultural applications. Technical details and considerations for realistic data synthesis and practical annotations have been discussed, and also, we have suggested potential agricultural tasks with active vision that could be explored using this dataset. Furthermore, our experimental results from fruit-search scenarios have been presented to demonstrate a specific use case.

For future work, we consider simulating a depth camera to curate 3D data, and other challenging plants for perception, such as walnut trees, along with larger-scale (e.g., multi-row) orchards could be included in the next version of dataset. Sim-to-real transfer could also be studied using this dataset.

REFERENCES

- [1] G. Kootstra, X. Wang, P. M. Blok, J. Hemming, and E. Van Henten, "Selective harvesting robotics: current research, trends, and future directions," *Current Robotics Reports*, vol. 2, pp. 95–104, 2021.
- [2] T. Choi, O. Would, A. Salazar-Gomez, and G. Cielniak, "Self-supervised representation learning for reliable robotic monitoring of fruit anomalies," in *2022 International Conference on Robotics and Automation (ICRA)*. IEEE, 2022, pp. 2266–2272.
- [3] A. G. Olenskyj, B. S. Sams, Z. Fei, V. Singh, P. V. Raja, G. M. Bornhorst, and J. M. Earles, "End-to-end deep learning for directly estimating grape yield from ground-based imagery," *Computers and Electronics in Agriculture*, vol. 198, p. 107081, 2022.
- [4] R. Bajcsy, "Active perception," *Proceedings of the IEEE*, vol. 76, no. 8, pp. 966–1005, 1988.
- [5] C. Lehnert, D. Tsai, A. Eriksson, and C. McCool, "3d move to see: Multi-perspective visual servoing towards the next best view within unstructured and occluded environments," in *2019 IEEE/RSJ International Conference on Intelligent Robots and Systems (IROS)*. IEEE, 2019, pp. 3890–3897.
- [6] R. van Essen, B. Harel, G. Kootstra, and Y. Edan, "Dynamic viewpoint selection for sweet pepper maturity classification using online economic decisions," *Applied Sciences*, vol. 12, no. 9, p. 4414, 2022.
- [7] T. Zaenker, C. Smitt, C. McCool, and M. Bennewitz, "Viewpoint planning for fruit size and position estimation," in *2021 IEEE/RSJ International Conference on Intelligent Robots and Systems (IROS)*. IEEE, 2021, pp. 3271–3277.
- [8] A. K. Burusa, E. J. van Henten, and G. Kootstra, "Attention-driven active vision for efficient reconstruction of plants and targeted plant parts," *arXiv preprint arXiv:2206.10274*, 2022.
- [9] X. Zeng, T. Zaenker, and M. Bennewitz, "Deep reinforcement learning for next-best-view planning in agricultural applications," in *2022 International Conference on Robotics and Automation (ICRA)*. IEEE, 2022, pp. 2323–2329.
- [10] R. Menon, T. Zaenker, and M. Bennewitz, "Viewpoint planning based on shape completion for fruit mapping and reconstruction," *arXiv preprint arXiv:2209.15376*, 2022.
- [11] P. Ammirato, P. Poirson, E. Park, J. Košecká, and A. C. Berg, "A dataset for developing and benchmarking active vision," in *2017 IEEE International Conference on Robotics and Automation (ICRA)*. IEEE, 2017, pp. 1378–1385.
- [12] Q. Zhao, L. Zhang, L. Wu, H. Qiao, and Z. Liu, "A real 3d embodied dataset for robotic active visual learning," *IEEE Robotics and Automation Letters*, vol. 7, no. 3, pp. 6646–6652, 2022.
- [13] B. N. Bailey, "Helios: A scalable 3d plant and environmental biophysical modeling framework," *Frontiers in Plant Science*, vol. 10, p. 1185, 2019.
- [14] J. Yang, Z. Ren, M. Xu, X. Chen, D. J. Crandall, D. Parikh, and D. Batra, "Embodied amodal recognition: Learning to move to perceive objects," in *Proceedings of the IEEE/CVF International Conference on Computer Vision*, 2019, pp. 2040–2050.
- [15] E. Safronov, N. Piga, M. Colledanchise, and L. Natale, "Active perception for ambiguous objects classification," in *2021 IEEE/RSJ International Conference on Intelligent Robots and Systems (IROS)*. IEEE, 2021, pp. 4437–4444.
- [16] F. Fang, W. Liang, Y. Wu, Q. Xu, and J.-H. Lim, "Self-supervised reinforcement learning for active object detection," *IEEE Robotics and Automation Letters*, vol. 7, no. 4, pp. 10224–10231, 2022.
- [17] R. Cheng, A. Agarwal, and K. Fragkiadaki, "Reinforcement learning of active vision for manipulating objects under occlusions," in *Conference on Robot Learning*. PMLR, 2018, pp. 422–431.
- [18] D. Nilsson, A. Pirinen, E. Gärtner, and C. Sminchisescu, "Embodied visual active learning for semantic segmentation," in *Proceedings of the AAAI Conference on Artificial Intelligence*, vol. 35, no. 3, 2021, pp. 2373–2383.
- [19] J. Zeng, Y. Li, Y. Ran, S. Li, F. Gao, L. Li, S. He, Q. Ye *et al.*, "Efficient view path planning for autonomous implicit reconstruction," *arXiv preprint arXiv:2209.13159*, 2022.
- [20] X. Ye, Z. Lin, H. Li, S. Zheng, and Y. Yang, "Active object perceiver: Recognition-guided policy learning for object searching on mobile robots," in *2018 IEEE/RSJ International Conference on Intelligent Robots and Systems (IROS)*. IEEE, 2018, pp. 6857–6863.
- [21] J. F. Schmid, M. Lauri, and S. Frintrop, "Explore, approach, and terminate: Evaluating subtasks in active visual object search based on deep reinforcement learning," in *2019 IEEE/RSJ International Conference on Intelligent Robots and Systems (IROS)*. IEEE, 2019, pp. 5008–5013.
- [22] Q. Xu, F. Fang, N. Gauthier, W. Liang, Y. Wu, L. Li, and J.-H. Lim, "Towards efficient multiview object detection with adaptive action prediction," in *2021 IEEE International Conference on Robotics and Automation (ICRA)*. IEEE, 2021, pp. 13423–13429.
- [23] S. Liu, G. Tian, Y. Zhang, M. Zhang, and S. Liu, "Active object detection based on a novel deep q-learning network and long-term learning strategy for the service robot," *IEEE Transactions on Industrial Electronics*, vol. 69, no. 6, pp. 5984–5993, 2021.
- [24] T. Hodan, P. Haluza, Š. Obdržálek, J. Matas, M. Lourakis, and X. Zabulis, "T-less: An rgb-d dataset for 6d pose estimation of texture-less objects," in *2017 IEEE Winter Conference on Applications of Computer Vision (WACV)*. IEEE, 2017, pp. 880–888.
- [25] A. Singh, J. Sha, K. S. Narayan, T. Achim, and P. Abbeel, "Bigbird: A large-scale 3d database of object instances," in *2014 IEEE international conference on robotics and automation (ICRA)*. IEEE, 2014, pp. 509–516.
- [26] J. Yang, Y. Gao, D. Li, and S. L. Waslander, "ROBI: A multi-view dataset for reflective objects in robotic bin-picking," in *2021 IEEE/RSJ International Conference on Intelligent Robots and Systems (IROS)*. IEEE, 2021, pp. 9788–9795.
- [27] A. Szot, A. Clegg, E. Undersander, E. Wijmans, Y. Zhao, J. Turner, N. Maestre, M. Mukadam, D. S. Chaplot, O. Maksymets *et al.*, "Habitat 2.0: Training home assistants to rearrange their habitat," *Advances in Neural Information Processing Systems*, vol. 34, pp. 251–266, 2021.
- [28] J. A. Gibbs, M. P. Pound, A. P. French, D. M. Wells, E. H. Murchie, and T. P. Pridmore, "Active vision and surface reconstruction for 3d plant shoot modelling," *IEEE/ACM Transactions on Computational Biology and Bioinformatics*, vol. 17, no. 6, pp. 1907–1917, 2019.
- [29] E. Rohmer, S. P. Singh, and M. Freese, "V-rep: A versatile and scalable robot simulation framework," in *2013 IEEE/RSJ international conference on intelligent robots and systems*. IEEE, 2013, pp. 1321–1326.
- [30] M. Goslin and M. R. Mine, "The panda3d graphics engine," *Computer*, vol. 37, no. 10, pp. 112–114, 2004.
- [31] M. Quigley, K. Conley, B. Gerkey, J. Faust, T. Foote, J. Leibs, R. Wheeler, A. Y. Ng *et al.*, "Ros: an open-source robot operating system," in *ICRA workshop on open source software*, vol. 3, no. 3.2. Kobe, Japan, 2009, p. 5.
- [32] N. Koenig and A. Howard, "Design and use paradigms for gazebo, an open-source multi-robot simulator," in *2004 IEEE/RSJ International Conference on Intelligent Robots and Systems (IROS)(IEEE Cat. No. 04CH37566)*, vol. 3. IEEE, 2004, pp. 2149–2154.
- [33] J. Weber and J. Penn, "Creation and rendering of realistic trees," in *Proceedings of the 22nd annual conference on*

- Computer graphics and interactive techniques*, 1995, pp. 119–128.
- [34] R. Kirk, M. Mangan, and G. Cielniak, “Robust counting of soft fruit through occlusions with re-identification,” in *Computer Vision Systems: 13th International Conference, ICVS 2021, Virtual Event, September 22-24, 2021, Proceedings 13*. Springer, 2021, pp. 211–222.
- [35] T. Zaenker, C. Lehnert, C. McCool, and M. Bennewitz, “Combining local and global viewpoint planning for fruit coverage,” in *2021 European Conference on Mobile Robots (ECMR)*. IEEE, 2021, pp. 1–7.
- [36] R. Polvara, S. M. Mellado, I. Hroob, G. Cielniak, and M. Hanheide, “Collection and evaluation of a long-term 4d agri-robotic dataset,” *arXiv preprint arXiv:2211.14013*, 2022.
- [37] L. P. Kaelbling, M. L. Littman, and A. W. Moore, “Reinforcement learning: A survey,” *Journal of artificial intelligence research*, vol. 4, pp. 237–285, 1996.
- [38] V. Mnih, K. Kavukcuoglu, D. Silver, A. Graves, I. Antonoglou, D. Wierstra, and M. Riedmiller, “Playing atari with deep reinforcement learning,” *arXiv preprint arXiv:1312.5602*, 2013.